Inorganic Chemistry

pubs.acs.org/IC Article

Coordination of Uranyl to the Redox-Active Calix[4]pyrrole Ligand

Greggory T. Kent, Jesse Murillo, Guang Wu, Skye Fortier, and Trevor W. Hayton*

Cite This: *Inorg. Chem.* 2020, 59, 8629–8634 Read Online

ACCESS | Metrics & More | Article Recommendations | Supporting Information

ABSTRACT: Reaction of $[Li(THF)]_4[L]$ (L = Me_8-calix[4]-pyrrole]) with 0.5 equiv of $[U^{VI}O_2Cl_2(THF)_2]_2$ results in formation of the oxidized calix[4]pyrrole product, $[Li(THF)]_2[L^{\Delta}]$ (**1**), concomitant with formation of reduced uranium oxide byproducts. Complex **1** can also be generated by reaction of $[Li(THF)]_4[L]$ with 1 equiv of I_2. We hypothesize that formation of **1** proceeds via formation of a highly oxidizing *cis*-uranyl intermediate, $[Li]_2[cis\text{-}U^{VI}O_2(calix[4]pyrrole)]$. To test this hypothesis, we explored the reaction of **1** with either 0.5 equiv of $[U^{VI}O_2Cl_2(THF)_2]_2$ or 1 equiv of $[U^{VI}O_2(OTf)_2(THF)_3]$, which affords the isostructural uranyl complexes, $[Li(THF)][U^{VI}O_2(L^{\Delta})Cl(THF)]$ (**2**) and $[Li(THF)][U^{VI}O_2(L^{\Delta})(OTf)(THF)]$ (**3**), respectively. In the solid state, **2** and **3** feature unprecedented uranyl-η^5-pyrrole interactions, making them rare examples of uranyl organometallic complexes. In addition, **2** and **3** exhibit some of the smallest O−U−O angles reported to date (**2**: 162.0(7) and 162.7(7)°; **3**: 164.5(5)°). Importantly, the O−U−O bending observed in these complexes suggests that the oxidation of $[Li(THF)]_4[L]$ does indeed occur via an unobserved *cis*-uranyl intermediate.

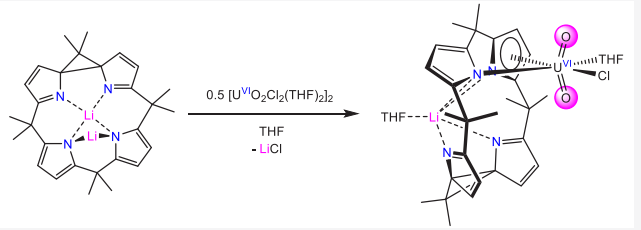

INTRODUCTION

The ability to manipulate the uranyl ($U^{VI}O_2^{2+}$) oxidation state has potential use in nuclear fuel processing, immobilization of uranyl contamination in groundwater, and uranium extraction from seawater.[1−6] Control of actinyl redox also has implications for the SANHEX process, which has been proposed as a method to separate Am and Cm from spent fuel.[7,8] Because of these potential applications, the redox chemistry of uranyl has come under increased scrutiny in recent years.[9,10] For example, in 2008, we reported the formation of $[U^{V}O_2(Ar_2nacnac)(Ph_2MePO)_2]$ ($Ar_2nacnac$ = (2,6-$^{i}Pr_2C_6H_3$)*N*C(Me)CHC(Me)*N*(2,6-$^{i}Pr_2C_6H_3$)) by reduction of $[U^{VI}O_2(Ar_2nacnac)(Ph_2MePO)_2][OTf]$ with Cp_2Co.[11] In this case, we argued that the normally unstable $U^{V}O_2^{+}$ ion was stabilized by the coordination of the strongly donating and sterically bulky $Ar_2nacnac$ ligand to the uranyl equatorial plane. Similarly, Mazzanti reported that reduction of $[U^{VI}O_2(dpaea)]$ ($dpaeaH_2$ = bis(pyridyl-6-methyl-2-carboxylate)-ethylamine) with Cp^*_2Co lead to formation of water-stable $[Cp^*_2Co][U^{V}O_2(dpaea)]$.[12] Another means of uranyl reduction, developed by us and others,[13−25] is "reductive silylation".[17,18] This technique has emerged as a reliable and general method for converting UO_2^{2+} to U^{5+} in nonaqueous environments—a transformation that is normally quite challenging.[10]

More recently, Bart and co-workers have shown that redox-active ligands can also mediate uranyl reduction and functionalization.[25−28] For example, treatment of the uranyl iminosemiquinone complex, $[(^{dipp}isq)_2U^{VI}O_2(THF)]$ (^{dipp}iq = 4,6-di-*tert*-butyl-2-[(2,6-diisopropylphenyl)imino]quinone) with pivaloyl chloride results in isolation of the U(IV) chloro complex, $[(^{dipp}iq)_2U^{IV}Cl_4]$, along with pivalic anhydride.[29] In this example, the two electrons required to convert U(VI) to U(IV) come from the iminosemiquinone ligand, which is converted to its neutral quinone form during the transformation. Similarly, we recently reported that reaction of $K_2(tmtaa)$ ($tmtaaH_2$ = dibenzotetramethyltetraaza[14]-annulene) with $[U^{VI}O_2Cl_2(THF)_2]_2$ resulted in formation of the $2e^-$ oxidation products of $(tmtaa)^{2-}$ (Scheme 1).[30] Also formed in the reaction is the reduced uranium oxide, U_4O_9. In this case, we hypothesized that the reaction products were formed upon decomposition of the unobserved *cis*-uranyl intermediate, *cis*-$[U^{VI}O_2(tmtaa)]$, which undergoes a facile intramolecular redox reaction. However, the hypothesized *cis*-uranyl intermediate has yet to be observed, which has limited our understanding of the role that uranyl structural changes play in mediating this redox chemistry. Moreover, this method of uranyl manipulation is still restricted to only a handful examples.[30−32]

In an effort to further develop this under-explored method of uranyl redox manipulation, we endeavored to study the ligation of other redox-active macrocycles to the uranyl ion. In this regard, the $[calix[4]pyrrole]^{4-}$ family of porphyrinogen macrocycles may be suitable candidates.[33,34] This ligand

Received: April 24, 2020
Published: June 3, 2020

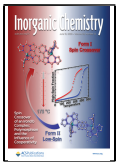

https://dx.doi.org/10.1021/acs.inorgchem.0c01224
Inorg. Chem. 2020, 59, 8629−8634

Scheme 1. Oxidation of $[tmtaa]^{2-}$ via the Proposed *cis*-Uranyl Intermediate, *cis*-$[U^{VI}O_2(tmtaa)]$

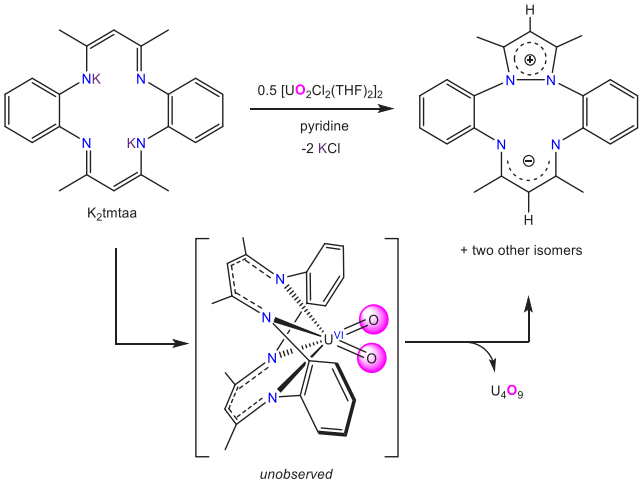

framework can exist in three different oxidation states, $[L]^{4-}$, $[L^{\Delta}]^{2-}$, and $L^{\Delta\Delta}$ (L = [Me_8-calix[4]pyrrole]$^{x-}$) (Chart 1).[33−36]

Chart 1. Chemical Structures of $[L]^{4-}$, $[L^{\Delta}]^{2-}$, and $L^{\Delta\Delta}$

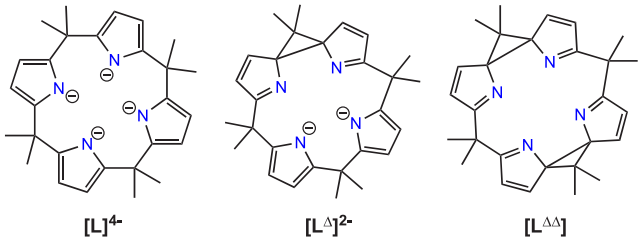

Moreover, these three states can be reversibly interconverted via chemical and electrochemical methods.[34] Given these past results, we hypothesized that ligation of $[L]^{4-}$ to uranyl would also result in metal reduction,[37,38] concomitant with ligand oxidation.

RESULTS AND DISCUSSION

Addition of 2 equiv. of $[Li(THF)]_4[L]$, as a colorless THF solution, to a THF solution of $[U^{VI}O_2Cl_2(THF)_2]_2$ results in an immediate color change from yellow to deep brown. Workup of the reaction mixture results in isolation of $[Li(THF)]_2[L^{\Delta}]$ (**1**) as orange blocks in 40% yield. Also formed in the reaction is a deep brown powder, which is likely uranium(IV) oxide per our past results with the $(tmtaa)^{2-}$ ligand (Scheme 2).[30] Complex **1** is the product of the $2e^-$ oxidation of $[calix[4]pyrrole]^{4-}$ by $[U^{VI}O_2Cl_2(THF)_2]_2$. As we hypothesized for our tmtaa chemistry,[30] we suggest that the reduction of uranyl to UO_2 proceeds via an unobserved, highly oxidizing *cis*-uranyl intermediate $[Li]_2[cis\text{-}U^{VI}O_2(calix[4]pyrrole)]$, which subsequently oxidizes the $[calix[4]pyrrole]^{4-}$ ligand. Similar results are observed upon reaction of $[Li(THF)]_4[L]$ with $[U^{VI}O_2Cl_2(Ph_3PO)_2]$ (see further discussion below).

X-ray quality crystals of **1** were grown by storage of a concentrated Et_2O solution for 24 h at −25 °C. When grown in this fashion, one of the coordinated THF molecules is partially replaced with a diethyl ether molecule, generating a material with the formula $[Li(THF)][Li(THF)_{0.58}(Et_2O)_{0.42}][L^{\Delta}]\cdot 0.5Et_2O$ (Figure 1). Its solid-state molecular structure

Scheme 2. Oxidation of $[Li(THF)]_4[L]$ with $[U^{VI}O_2Cl_2(THF)_2]_2$ or I_2

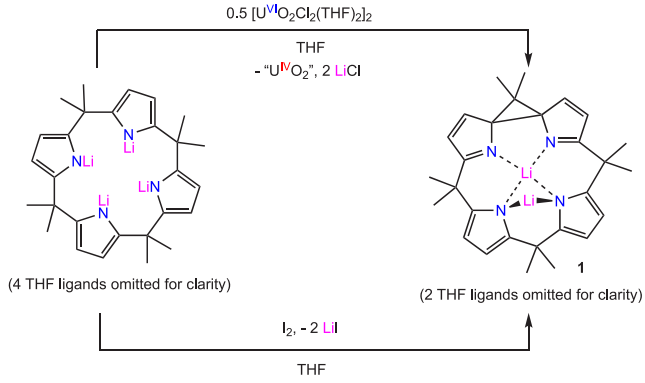

reveals the formation of a new carbon−carbon bond between two pyrrole rings (C15−C14 = 1.591(5) Å), resulting in the generation of a cyclopropyl ring. This structural change is further evidenced by the contraction of the oxidized dipyrrole subunit N−N distance (N3−N4 = 2.702(4) Å) relative to the reduced dipyrrole subunit N−N distance (N1−N2 = 2.887(4) Å). The oxidation state is further confirmed by the presence of only two lithium cations in the solid-state structure. One lithium cation is found in the inner cavity of the ring, bound to all four pyrrole nitrogen atoms and one molecule of THF, while the other lithium cation is found outside of the inner cavity and bound to two nitrogen atoms. Its third coordination site is occupied by a mixture of THF and Et_2O. The metrical parameters of **1** are in good agreement with those reported for other oxidized calix ligands, such as $[Li]_2[L'^{\Delta}]$ (L′ = Et_8-calix[4]pyrrole, i.e., the octaethyl-substituted analogue of the calix[4]pyrrole ligand)[35] and $[L^{\Delta}Zn]$.[34]

Complex **1** can also be accessed by reaction of $[Li(THF)]_4[L]$ with 1 equiv of I_2 in THF (Scheme 2). When synthesized in this fashion it can be isolated in 73% yield after workup. Its ^1H NMR spectrum in THF-d_8 at −60 °C features four pyrrole and six methyl environments, consistent with the C_s symmetry observed in the solid state (Figure S2). Curiously, upon warming to room temperature, the six methyl resonances coalesce into three broad, overlapping resonances, suggesting that the saddle structure of **1** undergoes rapid inversion at room temperature (Figure S1). Finally, the room-temperature $^7Li\{^1H\}$ NMR spectrum of **1** exhibits two broad resonances at 0.79 and −1.09 ppm, in a 1:1 ratio, which is also consistent with the solid-state structure (Figure S4).

In an effort to isolate a model structure of the proposed $[Li]_2[cis\text{-}U^{VI}O_2(calix[4]pyrrole)]$ intermediate, we explored the ligation of **1** to the uranyl fragment. We rationalized that, despite its increased rigidity due to the presence of the cyclopropyl ring, it should still be capable of binding to uranyl and provide a good approximation of the $[calix[4]pyrrole]^{4-}$ coordination environment. Moreover, because of its reduced oxidation potential relative to $[Li(THF)]_4[L]$,[34] we should not observe further uranyl redox chemistry. Thus, reaction of $[U^{VI}O_2Cl_2(THF)_2]_2$ with 2 equiv. of **1** in THF at −25 °C quickly results in a color change from yellow to deep green (Scheme 3). Workup of the reaction mixture, followed by crystallization from hexanes/toluene affords $[Li(THF)][U^{VI}O_2(L^{\Delta})Cl(THF)]$ (**2**), as deep green needles in 49% yield. Similarly, reaction of $[U^{VI}O_2(OTf)_2(THF)_3]$ with **1** in THF at −25 °C quickly results in a color change from yellow

https://dx.doi.org/10.1021/acs.inorgchem.0c01224
Inorg. Chem. 2020, 59, 8629−8634

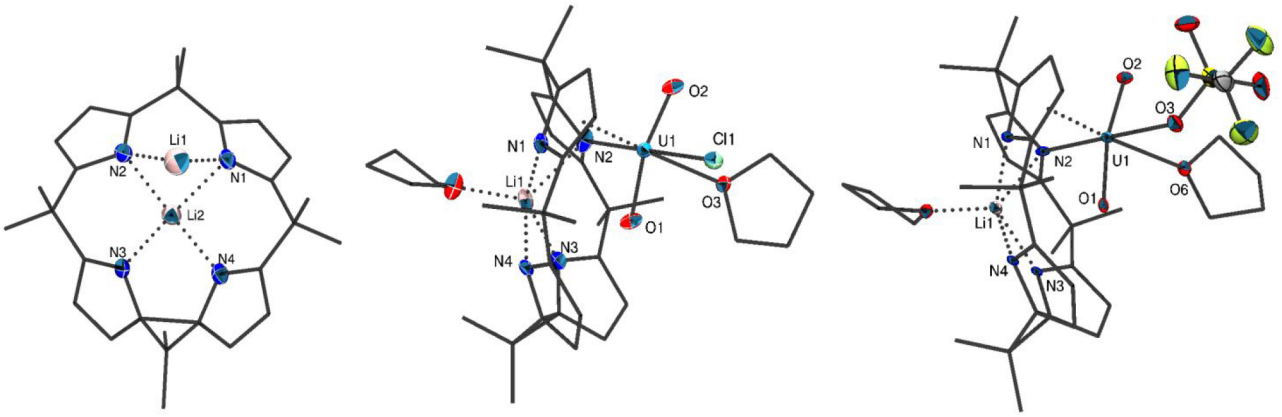

Figure 1. Solid-state molecular structures of complexes $[Li(THF)][Li(THF)_{0.58}(Et_2O)_{0.42}][L^{\Delta}]\cdot 0.5Et_2O$ (left), $[Li(THF)][U^{VI}O_2(L^{\Delta})Cl(THF)]\cdot C_7H_8$ (**2**·C_7H_8, middle), and $[Li(THF)][U^{VI}O_2(L^{\Delta})(OTf)(THF)]$ (**3**, right), respectively, with 50% probability ellipsoids shown for noncarbon atoms. Hydrogen atoms, solvate molecules, and coordinated Et_2O/THF molecules in $[Li(THF)][Li(THF)_{0.58}(Et_2O)_{0.42}][L^{\Delta}]\cdot 0.5Et_2O$ omitted for clarity.

Scheme 3. Synthesis of Complexes 2 and 3

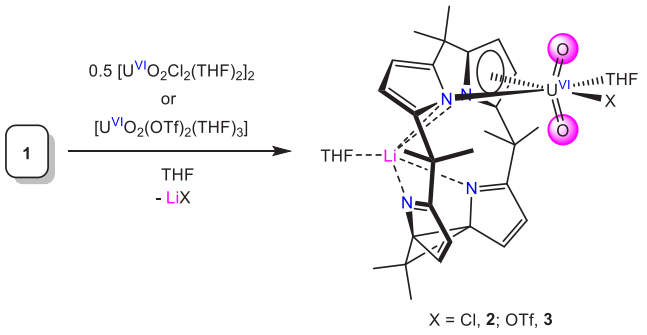

to deep green. Workup of the reaction mixture, followed by crystallization from THF, affords the analogous triflate complex, $[Li(THF)][U^{VI}O_2(L^{\Delta})(OTf)(THF)]$ (**3**), as deep green needles in 30% yield (Scheme 3). We attribute the lower yield of **3** to the accompanying formation of the fully oxidized calix fragment, $L^{\Delta\Delta}$, which we observe in the ^{1}H NMR spectra of the crude reaction mixtures (Figure S15).[34] The oxidation of $[L^{\Delta}]^{2-}$ to $L^{\Delta\Delta}$ during the reaction suggests that $[U^{VI}O_2(OTf)_2(THF)_3]$ is a better oxidant than $[U^{VI}O_2Cl_2(THF)_2]_2$, which is consistent with the weaker donor ability of $[OTf]^-$ vs $[Cl]^-$. Consistent with this hypothesis, $L^{\Delta\Delta}$ is not observed in crude reaction mixtures of **2**.

Complex **2** crystallizes in the triclinic space group $P\bar{1}$ as the toluene solvate, **2**·C_7H_8, with two independent molecules in the asymmetric unit, while complex **3** crystallizes in the monoclinic space group $P2_1/n$ (Figure 1). Complexes **2** and **3** are isostructural: both feature distorted octahedral geometries about the uranium center; however, **3** bears an κ^1-triflate group in place of the chloride ligand in **2**. The calix ligand in both complexes features a mixed η^1/η^5-binding mode to uranium, wherein the calix ligand binds to uranium via one pyrrole ring in an η^1-fashion and a second pyrrole ring in an η^5-fashion. A similar mixed-hapticity binding mode was observed in the U(III) complex, $[(Et_8\text{-calix[4] pyrrole})U^{III}(dme)][K(dme)]$.[39] Complexes **2** and **3** have U-centroid distances of 2.54(1) (U1−C4 = 2.716(19), U1−N1 = 2.771(16), U1−C3 = 2.836(18), U1−C1 = 2.84(2), U1−C2 = 2.871(19) Å) and 2.53(1) Å (U1−C2 = 2.690(6), U1−C3 = 2.771(6), U1−N1 = 2.792(5), U1−C4 = 2.870(6), U1−C5 = 2.923(6) Å), respectively. For comparison, the η^5-pyrrole interaction observed in **2** and **3** is reminiscent of the η^5-cyclopentadienyl interaction observed in $[NEt_4]_2[U^{VI}O_2(\eta^5\text{-}C_5Me_5)(CN)_3]$ and $(\eta^5\text{-}C_5Me_5)U^{VI}O_2(^{Mes}PDI^{Me})$ ($^{Mes}PDI^{Me}$ = 2,6-(2,4,6-Me_3-C_6H_2−N=CMe)$_2C_5H_3N$). These two complexes feature similar U-centroid distances of 2.598(3) and 2.582 Å, respectively.[25,40]

The average U=O bond lengths in **2** and **3** are 1.77 and 1.76 Å, respectively, which is typical of the *trans*-uranyl fragment.[11,41,42] However, the O−U−O angles in **2** (162.0(7)/162.7(7)°) and **3** (164.5(5)°) are substantially reduced from the 180° expected for this fragment, and are among the smallest reported to date (Table 1).[43,44] We attribute the O−U−O bending to the close approach of the ligand backbone to the O_{yl} atoms (**2**: O1···C25 = 2.82 Å and O2···C3 = 2.95 Å; **3**: O1···C9 = 2.84 Å and O2···C3 = 2.89 Å). Significantly, the O−U−O bending observed upon ligation of **1** to uranyl appears to confirm our hypothesis that the initial oxidation of [calix[4]-pyrrole]$^{4-}$ does, indeed, occur via a *cis*-uranyl intermediate. For comparison, the uranyl pyridinophane complexes, $[U^{VI}O_2(OTf)_2(^{H}N4)]$ and $[U^{VI}O_2(OTf)(THF)(^{Me}N4)][OTf]$ ($^{H}N4$ = 2,11-diaza[3,3](2,6) pyridinophane, and $^{Me}N4$ = *N*,*N*′-dimethyl-2,11-diaza[3,3](2,6) pyridinophane) feature O−U−O angles of 162.8(3)° and 161.7(5)°, respectively.[45] Similarly, the uranyl 1,10-phenanthroline (phen) complexes, $[U^{VI}O_2(phen)_2(2,4,6\text{-}X_3C_6H_2CO_2)_2]$ (X = F, Cl, Br), feature O−U−O angles ranging from 164.9(2)° to 162.2(2)°.[46] For further comparison, $[NEt_4]_2[U^{VI}O_2(\eta^5\text{-}$

Table 1. Selected Metrical Parameters for 2 and 3 (Å and deg)

	2	3
U=O	1.77(1)/1.78(1)	1.765(4)/1.762(4)
	1.77(2)/1.78(2)	
U−cent.	2.53(1)/2.54(1)	2.53(1)
$U-O_{THF}$	2.42(1)/2.45(2)	2.402(4)
U−X (X = Cl or OTf)	2.739(5)/2.736(4)	2.441(5)
U−N	2.54(1)/2.54(2)	2.494(5)
O−U−O (deg)	162.0(7)	164.5(5)
	162.7(7)	

https://dx.doi.org/10.1021/acs.inorgchem.0c01224
Inorg. Chem. 2020, 59, 8629−8634

$C_5Me_5)(CN)_3]$ and $(\eta^5$-$C_5Me_5)U^{VI}O_2(^{Mes}PDI^{Me})$, which feature similar η^5-bound rings, adopt O−U−O angles of 168.40(9)°,[40] and 168.3(2)°,[25] respectively. In all cases, bending can be rationalized by the steric constraints imposed by coordination of the ligand to the uranium center.[43] Finally, the lithium cations in both **2** and **3** are each coordinated to four N atoms of the calix ligand, as well as one THF molecule. This binding mode is reminiscent of the K^+ binding mode in $[(Et_8$-calix[4]tetrapyrrole$)U^{III}(dme)][K(dme)]$,[39] and the Li^+ binding mode in $[Li(THF)]_2[U^{VI}O_2(N(SiMe_3)_2)_2(tmtaa)]$.[47]

The ^{1}H NMR spectrum of **2** in THF-d_8 at −30 °C reveals eight doublets between 6.0 and 7.5 ppm, assignable to eight unique pyrrole environments, as well as eight singlets between 1.0 and 2.5 ppm, which are assignable to eight unique methyl environments (Figure S7), consistent with the C_1 symmetry seen in the solid state. However, upon warming **2** to 25 °C, the eight pyrrole and eight methyl environments coalesce and broaden significantly. This observation suggests that, at room temperature, the ligand fragment in **2** is rapidly exchanging its η^1- and η^5-bound pyrrole rings. The uranium-coordinated THF and $[Cl]^-$ ligands also likely undergo exchange. These parallel exchange processes result in an averaged structure that adequately rationalizes the room-temperature ^{1}H NMR spectrum. Similar dynamic behavior is observed for complex **3** (Figure S11). In addition, the $^{19}F\{^1H\}$ NMR spectrum of **3** features a sharp singlet at 78.43 ppm, assignable to the $[OTf]^-$ ligand (Figure S13), whereas the $^7Li\{^1H\}$ NMR spectrum of **3** features a broad peak at 0.02 ppm (Figure S12), which is assignable to the lone Li^+ environment. The $^7Li\{^1H\}$ NMR spectrum of **2** is essentially identical to that of **3** (Figure S9).

Finally, in an effort to probe the suitability of $[Li(THF)]_4[L]$ as a catalyst for uranyl reduction, we explored the chemical reversibility of the $[Li(THF)]_4[L]$ to **1** conversion. To that end, we monitored the reaction of $[Li(THF)]_4[L]$ with $[U^{VI}O_2Cl_2(Ph_3PO)_2]$ in THF-d_8 by ^{1}H NMR spectroscopy. This reaction results in an immediate color change from yellow to deep-brown. Additionally, no precipitate is observed to form. The ^{1}H NMR spectrum of the reaction mixture after 5 min revealed the presence of **1**, along with a small amount of H_4L. These two species are present in a 10:2 ratio. Subsequent addition of excess Li^0 to this sample resulted in complete disappearance of **1** and reformation of $[Li(THF)]_4[L]$ over the course of 10 h. The ratio of $[Li(THF)]_4[L]$:H_4L in this sample is 10:2.5 (Scheme 4 and Figure S16). On standing for 24 h, a deep-brown solid slowly began to deposit in the reaction mixture, which we ascribe to uranium(IV) oxide. Note that Floriani and co-workers previously reported reduction of $[Li]_2[L'^{\Delta}]$ with 2 equiv of Li^0 results in formation of $[Li]_4[L']$.[35] Overall, the reversibility of the $[Li(THF)]_4[L]$ oxidation suggest that it could be employed in the catalytic reduction of uranyl. However, its high water sensitivity renders it impractical for use in real-world systems. Nonetheless, our results represent an important proof-of-principle toward the development of a practical system.

Scheme 4. Reversible Redox Chemistry of 1

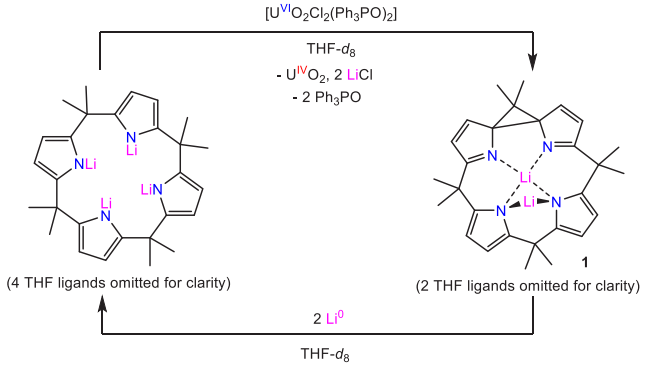

CONCLUSION

In summary, we have explored the reactivity of the well-known macrocyclic ligand, $[Li(THF)]_4[Me_8$-calix[4]pyrrole], with the uranyl ion. This reaction results in oxidation of the $[calix[4]pyrrole]^{4-}$ fragment, forming of the oxidized calix ligand, $[Li(THF)]_2[L^{\Delta}]$ (**1**), concomitant with reduction of the uranyl ion. We hypothesize that this reaction proceeds through a highly oxidizing *cis*-uranyl intermediate, $[Li]_2[cis$-$U^{VI}O_2(L)]$. In an effort to test this hypothesis, we explored the reaction of **1** with uranyl salts, which results in the isolation of $[Li(THF)][U^{VI}O_2(L^{\Delta})Cl(THF)]$ (**2**) and $[Li(THF)]$-$[U^{VI}O_2(L^{\Delta})(OTf)(THF)]$ (**3**). Significantly, complexes **2** and **3** are the first η^5-pyrrole complexes of the uranyl ion. As such, they represent rare examples of organometallic uranyl complexes.[25,40,48−55] Moreover, the O−U−O bending observed in the solid state for these two complexes supports our hypothesis that reduction of uranyl by $[Li(THF)]_4[Me_8$-calix[4]pyrrole] occurs via a *cis*-uranyl intermediate. Our results present the most detailed picture yet of the structural changes that occur to uranyl upon coordination to a macrocycle, and provide further support that O−U−O bending in the uranyl ion renders it a strong oxidant. In addition, this transformation represents a rare example of the controlled reduction of uranyl by ligation to a redox-active ligand. Going forward, we plan to develop this method of uranyl manipulation into an electrocatalytic uranyl reduction process.

ASSOCIATED CONTENT

Supporting Information

The Supporting Information is available free of charge at https://pubs.acs.org/doi/10.1021/acs.inorgchem.0c01224.

Experimental procedures and spectral data for complexes **1**−**3** (PDF)

Accession Codes

CCDC 1999046−1999048 contain the supplementary crystallographic data for this paper. These data can be obtained free of charge via www.ccdc.cam.ac.uk/data_request/cif, or by emailing data_request@ccdc.cam.ac.uk, or by contacting The Cambridge Crystallographic Data Centre, 12 Union Road, Cambridge CB2 1EZ, UK; fax: +44 1223 336033.

AUTHOR INFORMATION

Corresponding Author

Trevor W. Hayton − *Department of Chemistry and Biochemistry, University of California Santa Barbara, Santa Barbara, California 93106, United States;* orcid.org/0000-0003-4370-1424; Email: hayton@chem.ucsb.edu

Authors

Greggory T. Kent − *Department of Chemistry and Biochemistry, University of California Santa Barbara, Santa Barbara, California 93106, United States*

https://dx.doi.org/10.1021/acs.inorgchem.0c01224
Inorg. Chem. 2020, 59, 8629−8634

Jesse Murillo − *Department of Chemistry and Biochemistry, University of Texas at El Paso, El Paso, Texas 79968, United States*

Guang Wu − *Department of Chemistry and Biochemistry, University of California Santa Barbara, Santa Barbara, California 93106, United States*

Skye Fortier − *Department of Chemistry and Biochemistry, University of Texas at El Paso, El Paso, Texas 79968, United States;* orcid.org/0000-0002-0502-5229

Complete contact information is available at: https://pubs.acs.org/10.1021/acs.inorgchem.0c01224

Notes

The authors declare no competing financial interest.

■ ACKNOWLEDGMENTS

This work was supported by the U.S. Department of Energy, Office of Basic Energy Sciences, Chemical Sciences, Biosciences, and Geosciences Division, under Contract DE-SC-0001861. Crystallographic data for **2** were made possible by support from the NSF-MRI program (CHE-1827875).

■ REFERENCES

(1) Morris, D. E. Redox Energetics and Kinetics of Uranyl Coordination Complexes in Aqueous Solution. *Inorg. Chem.* **2002**, *41*, 3542−3547.

(2) Morrison, S. J.; Metzler, D. R.; Carpenter, C. E. Uranium Precipitation in a Permeable Reactive Barrier by Progressive Irreversible Dissolution of Zerovalent Iron. *Environ. Sci. Technol.* **2001**, *35*, 385−390.

(3) Lovley, D. R.; Phillips, E. J. P.; Gorby, Y. A.; Landa, E. R. Microbial Reduction of Uranyl. *Nature* **1991**, *350*, 413−416.

(4) Noubactep, C.; Meinrath, G.; Dietrich, P.; Merkel, B. Mitigating Uranium in Groundwater: Prospects and Limitations. *Environ. Sci. Technol.* **2003**, *37*, 4304−4308.

(5) Liu, C.; Hsu, P.-C.; Xie, J.; Zhao, J.; Wu, T.; Wang, H.; Liu, W.; Zhang, J.; Chu, S.; Cui, Y. A half-wave rectified alternating current electrochemical method for uranium extraction from seawater. *Nat. Energy* **2017**, *2*, 17007.

(6) Xu, Y.; Zondlo, J. W.; Finklea, H. O.; Brennsteiner, A. Electrosorption of uranium on carbon fibers as a means of environmental remediation. *Fuel Process. Technol.* **2000**, *68*, 189−208.

(7) McCann, K.; Brigham, D. M.; Morrison, S.; Braley, J. C. Hexavalent Americium Recovery Using Copper(III) Periodate. *Inorg. Chem.* **2016**, *55*, 11971−11978.

(8) McCann, K.; Mincher, B. J.; Schmitt, N. C.; Braley, J. C. Hexavalent Actinide Extraction Using *N*,*N*-Dialkyl Amides. *Ind. Eng. Chem. Res.* **2017**, *56*, 6515−6519.

(9) Arnold, P. L.; Love, J. B.; Patel, D. Pentavalent uranyl complexes. *Coord. Chem. Rev.* **2009**, *253*, 1973−1978.

(10) Cowie, B. E.; Purkis, J. M.; Austin, J.; Love, J. B.; Arnold, P. L. Thermal and Photochemical Reduction and Functionalization Chemistry of the Uranyl Dication, $[U^{VI}O_2]^{2+}$. *Chem. Rev.* **2019**, *119*, 10595−10637.

(11) Hayton, T. W.; Wu, G. Synthesis, Characterization, and Reactivity of a Uranyl β-Diketiminate Complex. *J. Am. Chem. Soc.* **2008**, *130*, 2005−2014.

(12) Faizova, R.; Scopelliti, R.; Chauvin, A.-S.; Mazzanti, M. Synthesis and Characterization of a Water Stable Uranyl(V) Complex. *J. Am. Chem. Soc.* **2018**, *140*, 13554−13557.

(13) Berthet, J.-C.; Siffredi, G.; Thuéry, P.; Ephritikhine, M. Controlled Chemical Reduction of Uranyl Salts into $UX_4(MeCN)_4$ (X = Cl, Br, I) with Me_3SiX Reagents. *Eur. J. Inorg. Chem.* **2007**, *2007*, 4017−4020.

(14) Arnold, P. L.; Jones, G. M.; Odoh, S. O.; Schreckenbach, G.; Magnani, N.; Love, J. B. Strongly coupled binuclear uranium−oxo complexes from uranyl oxo rearrangement and reductive silylation. *Nat. Chem.* **2012**, *4*, 221−227.

(15) Arnold, P. L.; Pécharman, A.-F.; Love, J. B. Oxo Group Protonation and Silylation of Pentavalent Uranyl Pacman Complexes. *Angew. Chem., Int. Ed.* **2011**, *50*, 9456−9458.

(16) Yahia, A.; Arnold, P. L.; Love, J. B.; Maron, L. The Effect of the Equatorial Environment on Oxo-Group Silylation of the Uranyl Dication: A Computational Study. *Chem. - Eur. J.* **2010**, *16*, 4881−4888.

(17) Arnold, P. L.; Pecharman, A.-F.; Hollis, E.; Yahia, A.; Maron, L.; Parsons, S.; Love, J. B. Uranyl oxo activation and functionalization by metal cation coordination. *Nat. Chem.* **2010**, *2*, 1056−1061.

(18) Arnold, P. L.; Patel, D.; Wilson, C.; Love, J. B. Reduction and selective oxo group silylation of the uranyl dication. *Nature* **2008**, *451*, 315−318.

(19) Schnaars, D. D.; Wu, G.; Hayton, T. W. Silylation of the Uranyl Ion Using $B(C_6F_5)_3$-Activated Et_3SiH. *Inorg. Chem.* **2011**, *50*, 9642−9649.

(20) Schnaars, D. D.; Wu, G.; Hayton, T. W. Borane-Mediated Silylation of a Metal-Oxo Ligand. *Inorg. Chem.* **2011**, *50*, 4695−4697.

(21) Brown, J. L.; Mokhtarzadeh, C. C.; Lever, J. M.; Wu, G.; Hayton, T. W. Facile Reduction of a Uranyl(VI) β-Ketoiminate Complex to U(IV) Upon Oxo Silylation. *Inorg. Chem.* **2011**, *50*, 5105−5112.

(22) Pedrick, E. A.; Wu, G.; Hayton, T. W. Oxo Ligand Substitution in a Cationic Uranyl Complex: Synergistic Interaction of an Electrophile and a Reductant. *Inorg. Chem.* **2015**, *54*, 7038−7044.

(23) Pedrick, E. A.; Wu, G.; Kaltsoyannis, N.; Hayton, T. W. Reductive Silylation of a Uranyl Dibenzoylmethanate Complex: An Example of Controlled Uranyl Oxo Ligand Cleavage. *Chem. Sci.* **2014**, *5*, 3204−3213.

(24) Pedrick, E. A.; Wu, G.; Hayton, T. W. Reductive Silylation of the Uranyl Ion with Ph_3SiOTf. *Inorg. Chem.* **2014**, *53*, 12237−12239.

(25) Kiernicki, J. J.; Cladis, D. P.; Fanwick, P. E.; Zeller, M.; Bart, S. C. Synthesis, Characterization, and Stoichiometric U−O Bond Scission in Uranyl Species Supported by Pyridine(diimine) Ligand Radicals. *J. Am. Chem. Soc.* **2015**, *137*, 11115−11125.

(26) Kiernicki, J. J.; Harwood, J. S.; Fanwick, P. E.; Bart, S. C. Reductive silylation of $Cp^*UO_2(^{Mes}PDI^{Me})$ promoted by Lewis bases. *Dalton Trans.* **2016**, *45*, 3111−3119.

(27) Kiernicki, J. J.; Zeller, M.; Bart, S. C. Facile Reductive Silylation of UO_2^{2+} to Uranium(IV) Chloride. *Angew. Chem., Int. Ed.* **2017**, *56*, 1097−1100.

(28) Coughlin, E.; Bart, S. C. Reductive silylation of uranyl mediated by iminosemiquinone ligands. *Polyhedron* **2019**, *170*, 783−787.

(29) Coughlin, E. J.; Qiao, Y.; Lapsheva, E.; Zeller, M.; Schelter, E. J.; Bart, S. C. Uranyl Functionalization Mediated by Redox-Active Ligands: Generation of O−C Bonds via Acylation. *J. Am. Chem. Soc.* **2019**, *141*, 1016−1026.

(30) Assefa, M. K.; Pedrick, E. A.; Wakefield, M. E.; Wu, G.; Hayton, T. W. Oxidation of the 14-Membered Macrocycle Dibenzotetramethyltetraaza[14]annulene upon Ligation to the Uranyl Ion. *Inorg. Chem.* **2018**, *57*, 8317−8324.

(31) Duval, P. B.; Burns, C. J.; Clark, D. L.; Morris, D. E.; Scott, B. L.; Thompson, J. D.; Werkema, E. L.; Jia, L.; Andersen, R. A. Synthesis and Structural Characterization of the First Uranium Cluster Containing an Isopolyoxometalate Core. *Angew. Chem., Int. Ed.* **2001**, *40*, 3357−3361.

(32) Cantat, T.; Graves, C. R.; Scott, B. L.; Kiplinger, J. L. Challenging the Metallocene Dominance in Actinide Chemistry with a Soft PNP Pincer Ligand: New Uranium Structures and Reactivity Patterns. *Angew. Chem., Int. Ed.* **2009**, *48*, 3681−3684.

(33) De Angelis, S.; Solari, E.; Floriani, C.; Chiesi-Villa, A.; Rizzoli, C. Solvent-dependent forms of lithiated 5,5,10,10,15,15,20,20-octaethylporphyrinogen in solution and in the solid state and reaction with tetrahydrofuran. *J. Chem. Soc., Dalton Trans.* **1994**, 2467−2469.

(34) Bachmann, J.; Nocera, D. G. Multielectron Chemistry of Zinc Porphyrinogen: A Ligand-Based Platform for Two-Electron Mixed Valency. *J. Am. Chem. Soc.* **2004**, *126*, 2829−2837.

(35) Jubb, J.; Floriani, C.; Chiesi-Villa, A.; Rizzoli, C. Redox chemistry of meso-octaethylporphyrinogen: formation and opening of a cyclopropane ring. *J. Am. Chem. Soc.* **1992**, *114*, 6571−6573.
(36) Piarulli, U.; Solari, E.; Floriani, C.; Chiesi-Villa, A.; Rizzoli, C. Redox Chemistry Associated with the Complexation of Vanadium(V) and Tungsten(VI) by meso-Octaethylporphyrinogen: Formation and Cleavage of Cyclopropane Units Functioning as Shuttles of Two Electrons. *J. Am. Chem. Soc.* **1996**, *118*, 3634−3642.
(37) Burn, A. G.; Nash, K. Electrochemical behavior of uranyl in anhydrous polar organic media. *Radiochim. Acta* **2017**, *105*, 513−522.
(38) Martinot, L.; Gubbels, F.; Michaux, C.; Nemeeger, C. Electrochemical Properties of Uranium in Acetonitrile and *ββ′* Oxydipropionitrile: Kinetics and Electrodeposition. *Radiochim. Acta* **1992**, *57*, 119−124.
(39) Korobkov, I.; Gambarotta, S.; Yap, G. P. A. A Highly Reactive Uranium Complex Supported by the Calix[4]tetrapyrrole Tetraanion Affording Dinitrogen Cleavage, Solvent Deoxygenation, and Polysilanol Depolymerization. *Angew. Chem., Int. Ed.* **2002**, *41*, 3433−3436.
(40) Maynadié, J.; Berthet, J.-C.; Thuéry, P.; Ephritikhine, M. The first cyclopentadienyl complex of uranyl. *Chem. Commun.* **2007**, 486−488.
(41) Wilkerson, M. P.; Burns, C. J.; Paine, R. T.; Scott, B. L. Synthesis and Crystal Structure of $UO_2Cl_2(THF)_3$: A Simple Preparation of an Anhydrous Uranyl Reagent. *Inorg. Chem.* **1999**, *38*, 4156−4158.
(42) Copping, R.; Jeon, B.; Pemmaraju, C. D.; Wang, S.; Teat, S. J.; Janousch, M.; Tyliszczak, T.; Canning, A.; Grønbech-Jensen, N.; Prendergast, D.; Shuh, D. K. Toward Equatorial Planarity about Uranyl: Synthesis and Structure of Tridentate Nitrogen-Donor $\{UO_2\}^{2+}$ Complexes. *Inorg. Chem.* **2014**, *53*, 2506−2515.
(43) Hayton, T. W. Understanding the origins of O_{yl}−U−O_{yl} bending in the uranyl (UO_2^{2+}) ion. *Dalton Trans.* **2018**, *47*, 1003−1009.
(44) Schöne, S.; Radoske, T.; März, J.; Stumpf, T.; Patzschke, M.; Ikeda-Ohno, A. $[UO_2Cl_2(phen)_2]$, a Simple Uranium(VI) Compound with a Significantly Bent Uranyl Unit (phen = 1,10-phenanthroline). *Chem. - Eur. J.* **2017**, *23*, 13574−13578.
(45) Pedrick, E. A.; Schultz, J. W.; Wu, G.; Mirica, L. M.; Hayton, T. W. Perturbation of the O−U−O Angle in Uranyl by Coordination to a 12-Membered Macrocycle. *Inorg. Chem.* **2016**, *55*, 5693−5701.
(46) Carter, K. P.; Kalaj, M.; Kerridge, A.; Ridenour, J. A.; Cahill, C. L. How to Bend the Uranyl Cation via Crystal Engineering. *Inorg. Chem.* **2018**, *57*, 2714−2723.
(47) Pedrick, E. A.; Assefa, M. K.; Wakefield, M. E.; Wu, G.; Hayton, T. W. Uranyl Coordination by the 14-Membered Macrocycle Dibenzotetramethyltetraaza[14]annulene. *Inorg. Chem.* **2017**, *56*, 6638−6644.
(48) Schettini, M. F.; Wu, G.; Hayton, T. W. Synthesis and reactivity of a uranyl-imidazolyl complex. *Chem. Commun.* **2012**, *48*, 1484−1486.
(49) Seaman, L. A.; Hrobárik, P.; Schettini, M. F.; Fortier, S.; Kaupp, M.; Hayton, T. W. A Rare Uranyl(VI)−Alkyl Ate Complex $[Li(DME)_{1.5}]_2[UO_2(CH_2SiMe_3)_4]$ and Its Comparison with a Homoleptic Uranium(VI)−Hexaalkyl. *Angew. Chem., Int. Ed.* **2013**, *52*, 3259−3263.
(50) Maity, A. K.; Ward, R. J.; Rupasinghe, D. M. R. Y. P.; Zeller, M.; Walensky, J. R.; Bart, S. C. Organometallic Uranyl Complexes Featuring a Carbodicarbene Ligand. *Organometallics* **2020**, *39*, 783−787.
(51) Tourneux, J.-C.; Berthet, J.-C.; Cantat, T.; Thuéry, P.; Mézailles, N.; Ephritikhine, M. Exploring the Uranyl Organometallic Chemistry: From Single to Double Uranium−Carbon Bonds. *J. Am. Chem. Soc.* **2011**, *133*, 6162−6165.
(52) Arnold, P. L.; Casely, I. J.; Turner, Z. R.; Carmichael, C. D. Functionalised Saturated-Backbone Carbene Ligands: Yttrium and Uranyl Alkoxy−Carbene Complexes and Bicyclic Carbene−Alcohol Adducts. *Chem. - Eur. J.* **2008**, *14*, 10415−10422.
(53) Oldham, J. W. J.; Oldham, S. M.; Scott, B. L.; Abney, K. D.; Smith, W. H.; Costa, D. A. Synthesis and structure of *N*-heterocyclic carbene complexes of uranyl dichloride. *Chem. Commun.* **2001**, 1348−1349.
(54) Sarsfield, M. J.; Helliwell, M.; Collison, D. The first uranyl−methine carbon bond; a complex with out-of-plane uranyl equatorial coordination. *Chem. Commun.* **2002**, 2264−2265.
(55) Mungur, S. A.; Liddle, S. T.; Wilson, C.; Sarsfield, M. J.; Arnold, P. L. Bent metal carbene geometries in amido N-heterocyclic carbene complexes. *Chem. Commun.* **2004**, 2738−2739.

https://dx.doi.org/10.1021/acs.inorgchem.0c01224
Inorg. Chem. 2020, 59, 8629−8634